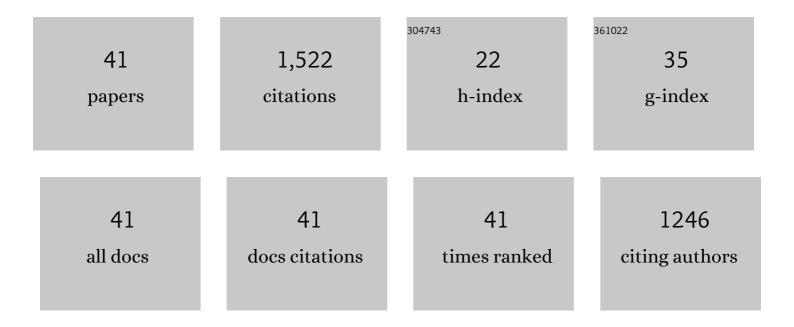
## Jean-Luc Froger

List of Publications by Year in descending order

Source: https://exaly.com/author-pdf/5288383/publications.pdf Version: 2024-02-01



#	Article	IF	CITATIONS
1	Volcano-wide fringes in ERS synthetic aperture radar interferograms of Etna (1992-1998): Deformation or tropospheric effect?. Journal of Geophysical Research, 2000, 105, 16391-16402.	3.3	147
2	Neogene ignimbrites of the Nevsehir plateau (Central Turkey): stratigraphy, distribution and source constraints. Journal of Volcanology and Geothermal Research, 1994, 63, 59-87.	2.1	143
3	Active spreading and regional extension at Mount Etna imaged by SAR interferometry. Earth and Planetary Science Letters, 2001, 187, 245-258.	4.4	130
4	Emplacement of volcanic vents and geodynamics of Central Anatolia, Turkey. Journal of Volcanology and Geothermal Research, 1998, 85, 33-54.	2.1	102
5	The deformation field of the August 2003 eruption at Piton de la Fournaise, Reunion Island, mapped by ASAR interferometry. Geophysical Research Letters, 2004, 31, .	4.0	77
6	Two scales of inflation at Lastarria-Cordon del Azufre volcanic complex, central Andes, revealed from ASAR-ENVISAT interferometric data. Earth and Planetary Science Letters, 2007, 255, 148-163.	4.4	70
7	Stratigraphy and age of the Cappadocia ignimbrites, Turkey: reconciling field constraints with paleontologic, radiochronologic, geochemical and paleomagnetic data. Journal of Volcanology and Geothermal Research, 2005, 141, 45-64.	2.1	68
8	Structure of Réunion Island (Indian Ocean) inferred from the interpretation of gravity anomalies. Journal of Volcanology and Geothermal Research, 1999, 88, 131-146.	2.1	64
9	Interpretation of anisotropy of magnetic susceptibility fabric of ignimbrites in terms of kinematic and sedimentological mechanisms: An Anatolian case-study. Earth and Planetary Science Letters, 1998, 157, 105-127.	4.4	58
10	Hidden calderas evidenced by multisource geophysical data; example of Cappadocian Calderas, Central Anatolia. Journal of Volcanology and Geothermal Research, 1998, 85, 99-128.	2.1	49
11	Insight into ground deformations at Lascar volcano (Chile) from SAR interferometry, photogrammetry and GPS data: Implications on volcano dynamics and future space monitoring. Remote Sensing of Environment, 2006, 100, 307-320.	11.0	47
12	Gravity structure of Piton de la Fournaise volcano and inferred mass transfer during the 2007 crisis. Journal of Volcanology and Geothermal Research, 2009, 184, 31-48.	2.1	47
13	Time-dependent displacements during and after the April 2007 eruption of Piton de la Fournaise, revealed by interferometric data. Journal of Volcanology and Geothermal Research, 2015, 296, 55-68.	2.1	47
14	Timing of a large volcanic flank movement at Piton de la Fournaise Volcano using noise-based seismic monitoring and ground deformation measurements. Geophysical Journal International, 2013, 195, 1132-1140.	2.4	43
15	Revised interpretation of recent InSAR signals observed at Llaima volcano (Chile). Geophysical Research Letters, 2015, 42, 3870-3879.	4.0	35
16	Hydrothermal and magmatic reservoirs at Lazufre volcanic area, revealed by a high-resolution seismic noise tomography. Earth and Planetary Science Letters, 2015, 421, 27-38.	4.4	34
17	Effusive crises at Piton de la Fournaise 2014–2015: a review of a multi-national response model. Journal of Applied Volcanology, 2017, 6, .	2.0	34
18	Long-term ground displacement observations using InSAR and GNSS at Piton de la Fournaise volcano between 2009 and 2014. Remote Sensing of Environment, 2017, 194, 230-247.	11.0	33

JEAN-LUC FROGER

#	Article	IF	CITATIONS
19	Magma Propagation at Piton de la Fournaise From Joint Inversion of InSAR and GNSS. Journal of Geophysical Research: Solid Earth, 2019, 124, 1361-1387.	3.4	33
20	Persistent uplift of the Lazufre volcanic complex (Central Andes): New insights from PCAIM inversion of InSAR time series and GPS data. Geochemistry, Geophysics, Geosystems, 2014, 15, 3591-3611.	2.5	32
21	Cointrusive shear displacement by sill intrusion in a detachment: A numerical approach. Geophysical Research Letters, 2014, 41, 1937-1943.	4.0	27
22	Assessing the reliability and consistency of InSAR and GNSS data for retrieving 3D-displacement rapid changes, the example of the 2015 Piton de la Fournaise eruptions. Journal of Volcanology and Geothermal Research, 2017, 344, 106-120.	2.1	24
23	Remote sensing of the 1998 mudflow at Casita volcano, Nicaragua. International Journal of Remote Sensing, 2003, 24, 4791-4816.	2.9	22
24	Inversion of coeval shear and normal stress of Piton de la Fournaise flank displacement. Journal of Geophysical Research: Solid Earth, 2016, 121, 7846-7866.	3.4	22
25	Monitoring an effusive eruption at Piton de la Fournaise using radar and thermal infrared remote sensing data: insights into the October 2010 eruption and its lava flows. Geological Society Special Publication, 2016, 426, 533-552.	1.3	22
26	The role of Interferometric Synthetic Aperture Radar in Detecting, Mapping, Monitoring, and Modelling the Volcanic Activity of Piton de la Fournaise, La Réunion: A Review. Remote Sensing, 2020, 12, 1019.	4.0	22
27	Multiscale framework for rapid change analysis from SAR image time series: Case study of flood monitoring in the central coast regions of Vietnam. Remote Sensing of Environment, 2022, 269, 112837.	11.0	17
28	Sheared sheet intrusions as mechanism for lateral flank displacement on basaltic volcanoes: Applications to Réunion Island volcanoes. Journal of Geophysical Research: Solid Earth, 2014, 119, 7607-7635.	3.4	15
29	Long-Term Subsidence in Lava Fields at Piton de la Fournaise Volcano Measured by InSAR: New Insights for Interpretation of the Eastern Flank Motion. Remote Sensing, 2018, 10, 597.	4.0	13
30	22 years of satellite imagery reveal a major destabilization structure at Piton de la Fournaise. Nature Communications, 2022, 13, 2649.	12.8	12
31	Variability of atmospheric precipitable water in northern Chile: Impacts on interpretation of InSAR data for earthquake modeling. Journal of South American Earth Sciences, 2011, 31, 214-226.	1.4	6
32	Combining InSAR and GNSS to Track Magma Transport at Basaltic Volcanoes. Remote Sensing, 2019, 11, 2236.	4.0	6
33	InSAR monitoring using RADARSAT-2 data at Piton de la Fournaise (La Reunion) and Karthala (Grande) Tj ETQq1	1 0,78431 1.3	.4 rgBT /Ove
34	Coherence Change Analysis for Multipass Insar Images Based on the Change Detection Matrix. , 2019, , .		5
35	The March–April 2007 Eruptions of Piton de la Fournaise as Recorded by Interferometric Data. Active Volcanoes of the World, 2016, , 271-286.	1.4	5
36	Multitemporal InSAR Coherence Change Analysis: Application to Volcanic Eruption Monitoring. , 2019,		3

#	Article	IF	CITATIONS
37	Mitigating bias in inversion of InSAR data resulting from radar viewing geometries. Geophysical Journal International, 2021, 227, 483-495.	2.4	2
38	Volcanic Eruption Monitoring Using Coherence Change Detection Matrix. , 2020, , .		1
39	SAR interferometry time series analysis of ground displacement for Piton de la Fournaise volcano, Reunion Island. , 2015, , .		Ο
40	Multiscale Change Analysis for SAR Image Time Series: Application to Inundation Detection. , 2019, , .		0
41	Influence of CNSS Configuration and Map Interpolation Method on INSAR Atmospheric Phase Assessment. , 2015, , .		0